Curl-conforming hierarchical vector bases for triangles and tetrahedra

Curl-Conforming Hierarchical Vector Bases for Triangles and Tetrahedra

Roberto D. Graglia, *Fellow, IEEE*, Andrew F. Peterson, *Fellow, IEEE*, and Francesco P. Andriulli, *Member, IEEE*

***Abstract*—A new family of hierarchical vector bases is proposed for triangles and tetrahedra. These functions span the curl-conforming reduced-gradient spaces of Nédélec. The bases are constructed from orthogonal scalar polynomials to enhance their linear independence, which is a simpler process than an orthogonalization applied to the final vector functions. Specific functions are tabulated to order 6.5. Preliminary results confirm that the new bases produce reasonably well-conditioned matrices.**

***Index Terms*—Basis functions, finite element methods, hierarchical basis functions, method of moments.**

I. INTRODUCTION

VECTOR basis functions find wide application in electromagnetics for volumetric discretizations of the vector Helmholtz equation in 2D and 3D and surface discretizations of the electric and magnetic field integral equations in 3D. These basis functions can be interpolatory, with coefficients that represent specific field components at interpolation points, or they can form hierarchical sets in order to facilitate adaptive refinement procedures. In contrast to interpolatory bases, hierarchical bases often exhibit poor linear independence as the order of the representation is increased, resulting in an ill-conditioned system of equations. In the following, a new hierarchical family of vector bases is proposed that alleviates the loss of linear independence.

Papers proposing hierarchical vector basis functions began appearing in the electromagnetics literature in the early 1990s. Most of the proposed basis functions are of the curl-conforming variety, which on triangles or quadrilaterals are easily converted into divergence-conforming functions. For brevity, we focus on curl-conforming bases on triangular and tetrahedral cells. Table I summarizes the existing curl-conforming hierarchical vector bases suitable for triangular or tetrahedral cells.

TABLE I
CLASSIFICATION OF HIERARCHICAL CURL-CONFORMING VECTOR-BASES AVAILABLE IN THE LITERATURE

Bases given in [ref.], year	Group	Element shapes		General formulas available	Explicit bases presented to degree
		2D	3D		
[3], 1993	A	none			2
[4], 1997	A	△	none	yes	
[5], 1997	A	△	none	yes	
[6], 1998 [7], 1999	B	△			2.5
[8], 1999	A	△			3
[9], 2001	A	none			3
[10], 2001	A	△ □	none	yes	
[11], 2003	A	none		yes	
[12], 2003	C	△	none		4.5
[13], 2004	C	△	none		4.5
[14], 2006	C	none			4.5
[15], 2005 [16], 2006	A	△ □	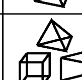	yes	
the present paper	B	△			6.5

The published hierarchical basis functions are here classified into three groups: (A) those that span complete polynomial vector spaces; (B) those that span the mixed-order spaces of Nédélec [1], and (C) those with subsets that exactly span both types of spaces. The procedure to obtain some of the bases considered in the Table is quite complex; for this reason the Table also shows the maximum polynomial degree of the bases explicitly reported in the relevant paper.

The published basis functions can be classified into three groups: A) those that span complete polynomial vector spaces, B) those that span the mixed-order spaces of Nédélec [1] (sometimes known as *reduced gradient* spaces for curl-conforming functions), and C) those with subsets that exactly span both types of spaces. As an example, the 1997 Graglia, Wilton, and Peterson interpolatory vector basis functions [2] fall into group B, since those basis functions span the mixed-order spaces of Nédélec but do not contain subsets that exactly span polynomial-complete spaces. The new hierarchical bases also belong to group B.

Although several families of bases appearing in Table I are considered to be "Nédélec" bases, here we classify them as "type A" because they do not contain subspaces that properly span the reduced-gradient spaces of [1] on triangles or tetrahedra. For instance, neither the face-based R_{30} functions of [8]

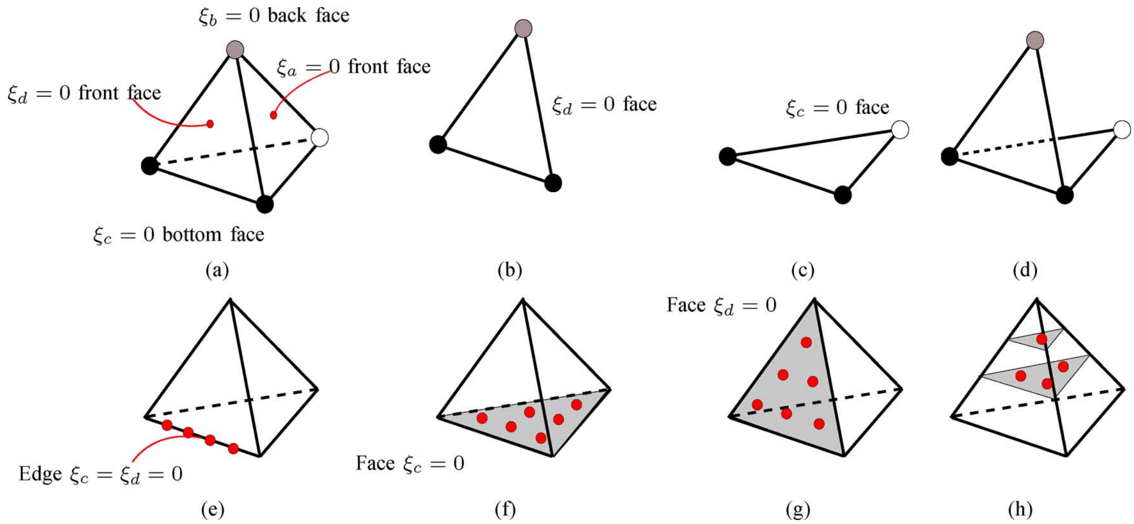

Fig. 1. The hierarchial polynomials that generate the curl-conforming functions associated with the zeroth-order vector function relative to the edge formed by the intersection of the $\xi_c = 0$ and $\xi_d = 0$ faces have features similar to those of the *equivalent* interpolatory polynomials in [2]. Vanishing regions: (a) the edge-based polynomials are different from zero on the cell boundaries; (b) all the polynomials based on the $\xi_c = 0$ face vanish on the face $\xi_d = 0$; (c) all the polynomials based on the $\xi_d = 0$ face vanish on the face $\xi_c = 0$; (d) the volume-based polynomials vanish on both the $\xi_c = 0$ and $\xi_d = 0$ faces. The number of hierarchical and interpolatory edge, face and volume-based polynomials of order p is the same. There are: (e) $(p+1)$ edge-based polynomials; (f, g) $p(p+1)/2$ polynomials based on the $\xi_c = 0$ and the $\xi_d = 0$ faces; (h) $p(p^2-1)/6$ volume-based polynomials. The figures from (e) to (h) show in red the interpolation nodes of the interpolatory polynomials for $p = 3$.

nor the R^3 functions of [9] properly span the Nédélec space of order 2.5; the "type 2" element-based functions of [15] do not properly span the Nédélec spaces of order 1.5 or higher. Thus these functions are listed here as belonging to type A.

Our new bases, first proposed in [17] and [18], have four distinguishing features: (a) the vector basis functions are subdivided from the outset into three different groups of edge, face, and volume-based functions; (b) each basis function is obtained by using one *generating* edge, face or volume-based polynomial whose analytical expression involves all the four dependent parent variables (ξ_a, ξ_b, ξ_c, ξ_d) that describe the tetrahedral element (notice that this holds even for the basis functions of the triangular element); (c) in each group, all the generating polynomials are mutually orthogonal independent of the definition domain of the inner product, i.e., either the volume, the face, or the edge of the tetrahedron; (d) the hierarchical vector functions are either symmetric or antisymmetric with respect to the parent variables that describe each edge and face of the cell.

The four features outlined above yield the following outcomes, respectively: (a) different individual polynomial orders can be used on each edge, face, and volumetric element of a given mesh, thereby facilitating the use of vector bases of different orders together in the same mesh (p-adaption); (b) the generating polynomials for the edge, the face, and the volume-based vector functions can be implemented in routines which can be used without modification to evaluate either the tetrahedral (for 3D codes) or the triangular (for 2D codes) vector functions; this greatly simplifies the implementation of the numerical codes required to deal with 3D or 2D structures; (c) our higher-order bases maintain excellent linear independence because they are derived after an *analytical* orthogonalization of the generating scalar polynomials, which is done in the element parent domain; (d) the procedure to enforce the conformity of the approximation across element interfaces is drastically simplified.

The outcome (c) is of importance because hierarchical bases are typically ill-conditioned at high orders and usually necessitate a cumbersome (partial) orthogonalization process to improve system conditioning. As illustrated by [19], considerable effort is required to directly orthogonalize the vector functions. In contrast, our bases are defined from orthogonal generating scalar polynomials, to enhance the conditioning of the system matrices. The outcome (d) is also of importance because enforcement of the continuity of the tangential component across adjacent elements (for the curl-conforming case) can be difficult [11], [20]; our basis functions reduce this problem to one of determining the correct sign of each basis function with respect to an arbitrarily selected reference direction along adjacent elements.

Our hierarchical vector functions are obtained by a three-step process. First, we orthogonalize on a given parent element appropriate linear combinations of the interpolatory scalar polynomials given in [2], to obtain hierarchical scalar polynomials. These polynomials are then multiplied by the zeroth-order vector functions of the element under consideration to obtain a set of vector functions. Finally, using a procedure similar to the one given in [2], any redundant basis function is eliminated from the resulting vector set.

II. Edge, Face, and Volume-Based Hierarchical Bases

The bases for the tetrahedral and the triangular cells are derived at the same time by simply considering the triangular cell described by the three parent variables (ξ_a, ξ_b, ξ_c) as the bounding ($\xi_d = 0$) face of the tetrahedral cell described by the four parent variables $\boldsymbol{\xi} = \{\xi_a, \xi_b, \xi_c, \xi_d\}$. Let us consider a tetrahedral element whose faces are labeled by these four parent variables and, at the same time, the triangular element defined by the $\xi_d = 0$ face of this tetrahedron (see Fig. 1). In terms of these parent variables, the zeroth-order curl-conforming vector-function *associated* with the edge in common to the

TABLE II

EDGE AND FACE-BASED HIERARCHICAL POLYNOMIALS UP TO THE SIXTH ORDER

Edge-based polynomials $E_p(\boldsymbol{\xi})$ of global order p, mutually orthogonal on the T^1, T^2 and T^3 simplex:	
$E_0^{ss} = P_0(\xi_{ab}) = 1$	$E_3^{as} = \sqrt{7}\,\{P_3(\xi_{ab}) - 3\,\chi_{cd}\,(\chi_{cd}-2)\,\xi_{ab}/2\}$
$E_1^{as} = \sqrt{3}\,\; P_1(\xi_{ab}) = \sqrt{3}\,\xi_{ab}$	$E_4^{ss} = \sqrt{9}\,\{P_4(\xi_{ab}) + 3\,\chi_{cd}\,(\chi_{cd}-2)\,\left(1+40\,\xi_a\,\xi_b - 9\,\chi_{ab}^2\right)/8\}$
$E_2^{ss} = \sqrt{5}\,\{P_2(\xi_{ab}) - \chi_{cd}\,(\chi_{cd}-2)\,/2\}$	$E_5^{as} = \sqrt{11}\,\{P_5(\xi_{ab}) + 5\,\chi_{cd}\,(\chi_{cd}-2)\,\xi_{ab}\,\left[3+56\,\xi_a\,\xi_b - 11\,\chi_{ab}^2\right]/8\}$
$E_6^{ss} = \sqrt{13}\,\{P_6(\xi_{ab}) - 5\,\chi_{cd}\,(\chi_{cd}-2)\,\left[1+43\,\chi_{ab}^4 + 84\,\xi_a\,\xi_b\,(1+12\,\xi_a\,\xi_b) - 20\,\chi_{ab}^2\,(1+21\,\xi_a\,\xi_b)\right]/16\}$	
Face-based polynomials $F_{mn}(\boldsymbol{\xi})$ of global order $p=(m+n)$, mutually orthogonal on the T^2 and T^3 simplex:	
$F_{01}^s = 2\sqrt{3}\,\xi_c$	$F_{05}^s = 2\sqrt{105}\,\xi_c\,\{66\,\xi_c^4 - 144\,\xi_c^3 + 108\,\xi_c^2 - 32\,\xi_c + 3 - \xi_d\,[3\,(1+\chi_{ab})$ $\times\,(1+\chi_{ab}^2) - \xi_c\,[29 + \chi_{ab}\,(26+23\,\chi_{ab})] + \xi_c^2\,(79+53\,\chi_{ab}) + 65\,\xi_c^3]\}$
$F_{02}^s = 2\sqrt{3}\,\xi_c\,(5\,\xi_c - 3 + 3\,\xi_d)$	$F_{14}^a = 6\sqrt{70}\,\xi_c\,\xi_{ab}\,\{33\,{\xi_c}^3 - 45\,{\xi_c}^2 + 18\,\xi_c - 2$ $+\xi_d\,[2\,(1+\chi_{ab}^2 + \chi_{ab}\,(1-7\,\xi_c)) - 16\,\xi_c + 29\,{\xi_c}^2]\}$
$F_{11}^a = 6\sqrt{5}\,\xi_c\,\xi_{ab}$	$F_{23}^s = 6\sqrt{10}\,\xi_c\,\chi_2\,\left[55\,{\xi_c}^2 - 40\,\xi_c + 6 + 2\xi_d\,(3\xi_d + 20\xi_c - 6)\right]$
$F_{03}^s = 2\sqrt{30}\,\xi_c\,\left[7\,\xi_c^2 - 8\,\xi_c + 2\right.$ $\left.+2\,\xi_d\,(4\,\xi_c - 2 + \xi_d)\right]$	$F_{32}^a = 6\sqrt{35}\,\xi_c\,\chi_3\,(11\,\xi_c - 3 + 3\xi_d)$
$F_{12}^a = 2\sqrt{30}\,\xi_c\,\xi_{ab}\,(7\,\xi_c - 3 + 3\,\xi_d)$	$F_{41}^s = 6\sqrt{165}\,\xi_c\,\chi_4$
$F_{21}^s = 2\sqrt{210}\,\xi_c\,\chi_2$	$F_{06}^s = 2\sqrt{42}\,\xi_c\,\{429\,{\xi_c}^5 - 1155\,{\xi_c}^4 + 1155\,\xi_c^3 - 525\,{\xi_c}^2 + 105\,\xi_c - 7$ $+7\,\xi_d\,\left[1+\chi_{ab}+\chi_{ab}^2+\chi_{ab}^3+\chi_{ab}^4 - (14+13\,\chi_{ab}+12\,\chi_{ab}^2+11\,\chi_{ab}^3)\,\xi_c\right.$ $\left.+(61+48\,\chi_{ab}+36\,\chi_{ab}^2)\,{\xi_c}^2 - 8\,(13+7\,\chi_{ab})\xi_c^3 + 61\,\xi_c^4\right]\}$
$F_{04}^s = 2\sqrt{15}\,\xi_c\,\{42\,{\xi_c}^3 - 70\,{\xi_c}^2$ $+35\,\xi_c - 5 + 5\,\xi_d\,[1+\chi_{ab}$ $+\chi_{ab}^2 - \xi_c\,(6+5\,\chi_{ab} - 8\,\xi_c)]\}$	$F_{15}^a = 6\sqrt{70}\,\xi_c\,\xi_{ab}\,\{143\,\xi_c^4 - 264\,\xi_c^3 + 165\,\xi_c^2 - 40\,\xi_c + 3 + \xi_d\,[136\,\xi_c^3 - 3$ $\times(1+\chi_{ab}+\chi_{ab}^2+\chi_{ab}^3) + (37+34\,\chi_{ab}+31\,\chi_{ab}^2)\,\xi_c - 2\,(64+47\,\chi_{ab})\,\xi_c^2]\}$
$F_{13}^a = 2\sqrt{105}\,\xi_c\,\xi_{ab}\,\left[18\,{\xi_c}^2 - 16\,\xi_c\right.$ $\left.+3 - \xi_d\,(3+3\,\chi_{ab} - 13\,\xi_c)\right]$	$F_{24}^s = 6\sqrt{35}\,\xi_c\,\chi_2\,\{143\,\xi_c^3 - 165\,\xi_c^2 + 55\,\xi_c - 5$ $+5\,\xi_d\,[1+\chi_{ab}+\chi_{ab}^2 - (10+9\,\chi_{ab})\,\xi_c + 23\,{\xi_c}^2]\}$
	$F_{33}^a = 14\sqrt{165}\,\xi_c\,\chi_3\,\left[13\,{\xi_c}^2 - 8\,\xi_c + 1 - \xi_d\,(2 - 8\,\xi_c - \xi_d)\right]$
$F_{22}^s = 10\sqrt{42}\,\xi_c\,\chi_2\,(3\,\xi_c - 1 + \xi_d)$	$F_{42}^s = 6\sqrt{77}\,\xi_c\,\chi_4\,(13\,\xi_c - 3 + 3\,\xi_d)$
$F_{31}^a = 6\sqrt{70}\,\xi_c\,\chi_3$	$F_{51}^a = 2\sqrt{3003}\,\xi_c\,\chi_5$

With $\xi_{ab} = \xi_a - \xi_b$; $\chi_{ab} = \xi_a + \xi_b$, and $\chi_{cd} = \xi_c + \xi_d$. Several equivalent polynomial expressions are obtained by using the dependency relation $\xi_a + \xi_b + \xi_c + \xi_d = 1$. The reported expressions were indeed made more compact by using the dependency relation and by setting:

$$\chi_2 = {\xi_a}^2 - 4\,\xi_a\,\xi_b + {\xi_b}^2\,; \qquad \chi_4 = {\xi_a}^4 - 16\,{\xi_a}^3\,\xi_b + 36\,{\xi_a}^2\,{\xi_b}^2 - 16\,\xi_a\,{\xi_b}^3 + {\xi_b}^4\,;$$

$$\chi_3 = \xi_{ab}\,\left({\xi_a}^2 - 8\,\xi_a\,\xi_b + {\xi_b}^2\right); \quad \chi_5 = \xi_{ab}\,\left({\xi_a}^4 - 24\,{\xi_a}^3\,\xi_b + 76\,{\xi_a}^2\,{\xi_b}^2 - 24\,\xi_a\,{\xi_b}^3 + {\xi_b}^4\right).$$

The first superscript s and a labels symmetric and antisymmetric polynomials of the ξ_a and ξ_b variables, respectively; the second superscript s, used only for E_p, indicates that the edge-based polynomials are symmetric in the ξ_c and ξ_d variables. The Table reports only the edge- and the face-based polynomials associated with the $\xi_c = \xi_d = 0$ edge and with the $\xi_d = 0$ face, respectively. The face-based polynomials associated with the $\xi_c = 0$ face of the tetrahedral element T^3 are obtained by interchanging ξ_c with ξ_d in the reported expressions. The polynomials for the triangular element T^2 are obtained by setting $\xi_d = 0$. Along its associated edge, E_p behaves as the Legendre polynomial $P_p(\xi_{ab})$ of order p. These polynomials are normalized as follows (where p indicates the global order of the polynomial, equal to the sum of its subscripts).

$$\int_{T^1} E_p^2(\boldsymbol{\xi})\,\mathrm{d}T^1 = 1\,; \quad \iint_{T^2} E_p^2(\boldsymbol{\xi})\,\mathrm{d}T^2 = \frac{1}{2p+2}\,; \quad \iiint_{T^3} E_p^2(\boldsymbol{\xi})\,\mathrm{d}T^3 = \frac{1}{(2p+2)(2p+3)}$$

$$\iint_{T^2} F_p^2(\boldsymbol{\xi})\,\mathrm{d}T^2 = 1\,; \qquad \iiint_{T^3} F_p^2(\boldsymbol{\xi})\,\mathrm{d}T^3 = \frac{1}{2p+3}$$

$\xi_c = 0$ and $\xi_d = 0$ face reads $\boldsymbol{\Omega}_{cd}(\boldsymbol{r}) = (\xi_b\,\boldsymbol{\nabla}\xi_a - \xi_a\,\boldsymbol{\nabla}\xi_b)$ and $\boldsymbol{\Omega}_c(\boldsymbol{r}) = -(\xi_b\,\boldsymbol{\nabla}\xi_a - \xi_a\,\boldsymbol{\nabla}\xi_b)$ for the tetrahedral and the triangular element, respectively [2]. Despite of the sign difference in the previous two expressions, which can be eventually eliminated by reorienting the triangle unit normal, both functions turn out to be antisymmetric with respect to the two parent variables ξ_a and ξ_b, since $\boldsymbol{\Omega}_{cd}(\xi_a,\ \xi_b) = -\boldsymbol{\Omega}_{cd}(\xi_b,\ \xi_a)$ and $\boldsymbol{\Omega}_c(\xi_a,\ \xi_b) = -\boldsymbol{\Omega}_c(\xi_b, \xi_a)$. Because of this property, the enforcement of the tangential continuity of the field across element boundaries is greatly simplified. The continuity of the tangential component is ensured by adjusting the basis function sign to correspond to an arbitrarily selected reference direction along the adjacent elements [2].

Higher order interpolatory bases are constructed in [2] by multiplying the zeroth-order vector functions with Silvester-Lagrange interpolatory polynomials. Here, linear combinations of those interpolatory polynomials are used to obtain symmetric or antisymmetric hierarchical scalar polynomials which, within each group, are constructed *a priori* to be mutually orthogonal.

Our hierarchical vector functions are constructed using the same technique given in [2], where we simply *substitute* the new scalar hierarchical polynomials for the interpolatory ones of [2].

With reference to Fig. 1, the interpolatory polynomials which in [2] are *associated* with the edge at the intersection of the $\xi_c = 0$ and $\xi_d = 0$ faces are subdivided into four different groups. The first group is formed by all the polynomials inter-

TABLE III

VOLUME-BASED HIERARCHICAL POLYNOMIALS $V_{ijk} = \xi_c\, \xi_d\, \mathcal{U}_{i-2,j,k}$ UP TO THE SIXTH ORDER

$\mathcal{U}_{000}^{ss} = 6\sqrt{35}$	$\mathcal{U}_{100}^{ss} = 6\sqrt{105}\,(4\,\chi_{ab} - 1)$
$\mathcal{U}_{200}^{ss} = 12\sqrt{55}\,(1 + 3\,\chi_{ab}\,(5\,\chi_{ab} - 3))$	$\mathcal{U}_{010}^{as} = 36\sqrt{35}\,\xi_{ab}$
$\mathcal{U}_{110}^{as} = 6\sqrt{2310}\,\xi_{ab}\,(5\,\chi_{ab} - 2)$	$\mathcal{U}_{001}^{sa} = 12\sqrt{105}\,\xi_{cd}$
$\mathcal{U}_{020}^{ss} = 15\sqrt{462}\,\left(3\,\xi_{ab}^2 - \chi_{ab}^2\right)$	$\mathcal{U}_{400}^{ss} = 30\,(5 + 11\,\chi_{ab}\,(-10 + \chi_{ab}\,(60 + 13\,\chi_{ab}\,(7\,\chi_{ab} - 10))))$
$\mathcal{U}_{101}^{sa} = 6\sqrt{1155}\,\xi_{cd}\,(5\,\chi_{ab} - 1)$	$\mathcal{U}_{310}^{as} = 90\sqrt{22}\,\xi_{ab}\,(-5 + \chi_{ab}\,(45 + 13\,\chi_{ab}\,(7\,\chi_{ab} - 9)))$
$\mathcal{U}_{011}^{aa} = 60\sqrt{231}\,\xi_{ab}\,\xi_{cd}$	$\mathcal{U}_{220}^{ss} = 30\sqrt{1155}\,(3 - 13\,\chi_{cd}\,\chi_{ab})\,\left(3\,\xi_{ab}^2 - \chi_{ab}^2\right)$
$\mathcal{U}_{002}^{ss} = 15\sqrt{11}\,\left(7\,\xi_{cd}^2 - \chi_{cd}^2\right)$	$\mathcal{U}_{130}^{as} = 15\sqrt{3003}\,\xi_{ab}\,(7\,\chi_{ab} - 4)\,\left(5\,\xi_{ab}^2 - 3\,\chi_{ab}^2\right)$
$\mathcal{U}_{300}^{ss} = 6\sqrt{390}\,(5\,\chi_{ab}\,(3 - 11\,\chi_{cd}\,\chi_{ab}) - 1)$	$\mathcal{U}_{040}^{ss} = 45\sqrt{1001}\,\left(3\,\chi_{ab}^4 - 30\,\chi_{ab}^2\,\xi_{ab}^2 + 35\,\xi_{ab}^4\right)/4$
$\mathcal{U}_{210}^{as} = 6\sqrt{390}\,\xi_{ab}\,(10 + 11\,\chi_{ab}\,(6\,\chi_{ab} - 5))$	$\mathcal{U}_{301}^{sa} = 30\sqrt{154}\,\xi_{cd}\,(-1 + \chi_{ab}\,(18 + 13\,\chi_{ab}\,(7\,\chi_{ab} - 6)))$
$\mathcal{U}_{120}^{ss} = 15\sqrt{6006}\,(2\,\chi_{ab} - 1)\,\left(3\,\xi_{ab}^2 - \chi_{ab}^2\right)$	$\mathcal{U}_{211}^{aa} = 30\sqrt{231}\,\xi_{ab}\,\xi_{cd}\,(10 + 13\,\chi_{ab}\,(7\,\chi_{ab} - 5))$
$\mathcal{U}_{030}^{as} = 6\sqrt{15015}\,\xi_{ab}\,\left(5\,\xi_{ab}^2 - 3\,\chi_{ab}^2\right)$	$\mathcal{U}_{121}^{sa} = 15\sqrt{15015}\,\xi_{cd}\,(7\,\chi_{ab} - 3)\,\left(3\,\xi_{ab}^2 - \chi_{ab}^2\right)$
$\mathcal{U}_{201}^{sa} = 30\sqrt{91}\,\xi_{cd}\,(1 + 11\,\chi_{ab}\,(2\,\chi_{ab} - 1))$	$\mathcal{U}_{031}^{aa} = 210\sqrt{429}\,\xi_{ab}\,\xi_{cd}\,\left(5\,\xi_{ab}^2 - 3\,\chi_{ab}^2\right)$
$\mathcal{U}_{111}^{aa} = 30\sqrt{6006}\,\xi_{ab}\,\xi_{cd}\,(3\,\chi_{ab} - 1)$	$\mathcal{U}_{202}^{ss} = 15\sqrt{6}\,(3 + 13\,\chi_{ab}\,(7\,\chi_{ab} - 3))\,\left(7\,\xi_{cd}^2 - \chi_{cd}^2\right)$
$\mathcal{U}_{021}^{sa} = 30\sqrt{3003}\,\xi_{cd}\,\left(3\,\xi_{ab}^2 - \chi_{ab}^2\right)$	$\mathcal{U}_{112}^{as} = 45\sqrt{143}\,\xi_{ab}\,(7\,\chi_{ab} - 2)\,\left(7\,\xi_{cd}^2 - \chi_{cd}^2\right)$
$\mathcal{U}_{102}^{ss} = 3\sqrt{715}\,(6\,\chi_{ab} - 1)\,\left(7\,\xi_{cd}^2 - \chi_{cd}^2\right)$	$\mathcal{U}_{022}^{ss} = 15\sqrt{15015}\,\left(\chi_{ab}^2 - 3\,\xi_{ab}^2\right)\left(\chi_{cd}^2 - 7\,\xi_{cd}^2\right)/2$
$\mathcal{U}_{012}^{as} = 15\sqrt{858}\,\xi_{ab}\,\left(7\,\xi_{cd}^2 - \chi_{cd}^2\right)$	$\mathcal{U}_{103}^{sa} = 15\sqrt{1001}\,\xi_{cd}\,(7\,\chi_{ab} - 1)\,\left(3\,\xi_{cd}^2 - \chi_{cd}^2\right)$
$\mathcal{U}_{003}^{sa} = 3\sqrt{10010}\,\xi_{cd}\,\left(3\,\xi_{cd}^2 - \chi_{cd}^2\right)$	$\mathcal{U}_{013}^{aa} = 105\sqrt{858}\,\xi_{ab}\,\xi_{cd}\,\left(3\,\xi_{cd}^2 - \chi_{cd}^2\right)$
	$\mathcal{U}_{004}^{ss} = 105\sqrt{13}\,\left(\chi_{cd}^4 - 18\,\chi_{cd}^2\,\xi_{cd}^2 + 33\,\xi_{cd}^4\right)/(4\sqrt{2})$

The Table reports the functions $\mathcal{U}_{\ell mn}$ up to the order $(\ell+m+n) = 4$. These functions form the set of the volume-based polynomials $V_{ijk} = \xi_c\,\xi_d\,\mathcal{U}_{i-2,j,k}$ up to the sixth-order. It is understood that $\xi_a + \xi_b + \xi_c + \xi_d = 1$; $\xi_{ab} = \xi_a - \xi_b$; $\xi_{cd} = \xi_c - \xi_d$; $\chi_{ab} = \xi_a + \xi_b$; $\chi_{cd} = \xi_c + \xi_d$. All the volume-based polynomials are mutually orthogonal on the T^3 simplex and are normalized to get $\iiint_{T^3} V_p^2(\boldsymbol{\xi})\,\mathrm{d}T^3 = 1$, where p is the global order of the volume polynomial, equal to the sum of its subscripts.

polating (up to a given order) at the edge (Fig. 1(e)) and that (in general) do not vanish on the other tetrahedral boundaries (Fig. 1(a)); a second group is formed by the polynomials that interpolate (up to a given order) at the $\xi_c = 0$ face (Fig. 1(f)) and that vanish on the face $\xi_d = 0$ (Fig. 1(b)); a third group is given by polynomials which interpolate at the $\xi_d = 0$ face (Fig. 1(g)) and vanish on $\xi_c = 0$ (Fig. 1(c)); the last group is given by the remaining interpolating polynomials which vanish on both the $\xi_c = 0$ and $\xi_d = 0$ faces (Fig. 1(d), (h)). Appropriate linear combinations of these interpolatory polynomials, together with extensive symmetry considerations, provide four groups of orthogonal hierarchical polynomials. These polynomials, derived and normalized in the Appendix, are explicitly reported in Tables II and III up to the sixth order. We have obtained hierarchical families up to eleventh order with this approach.

In Tables II–III, the first superscript s or a labels symmetric or antisymmetric polynomials of the ξ_a and ξ_b variables, respectively; similarly, the second superscript (used only for the edge- and the volume-based polynomials) labels symmetric and antisymmetric polynomials of the ξ_c and ξ_d variables.

All the edge-based hierarchical polynomials E_p of Table II are symmetric in the ξ_c and ξ_d variables. In Table II, $P_p(\xi_{ab})$ indicates the Legendre polynomial of order p, with $\xi_{ab} = \xi_a - \xi_b$. The polynomials based on the edge $\xi_c = 0$ of the T^2 simplex (triangular element, with $\xi_a + \xi_b + \xi_c = 1$) are obtained by setting $\xi_d = 0$. For the T^3 simplex (tetrahedral element, with $\xi_a + \xi_b + \xi_c + \xi_d = 1$), the polynomials reported are those based on the edge $\xi_c = 0$, $\xi_d = 0$. Along its associated edge, E_p behaves as the Legendre polynomial $P_p(\xi_{ab})$.

For the face-based polynomials of Table II one has to set $\xi_d = 0$ while dealing with the T^2 simplex; for the T^3 simplex, the polynomials reported are those associated with the $\xi_d = 0$ face.

Notice that the edge-based hierarchical polynomials of Table II are orthogonal on the T^1, T^2, and T^3 simplexes, while the face-based polynomials are orthogonal on both the T^2 and T^3 simplexes.

The number of Degrees of Freedom (DoF) for curl-conforming bases of order p on a tetrahedron is $(p+1)(p+3)(p+4)/2$; the number of DoFs for curl- and divergence-conforming bases of order p on a triangle is $(p+1)(p+3)$[2]. By following the same procedure reported in [2], the $p(p^2-1)/2$ elements of an order p hierarchical vector base associated with DoFs internal to the tetrahedral element $\mathcal{T}^3(\xi_a, \xi_b, \xi_c, \xi_d)$ are obtained by forming the product of the $p(p^2-1)/6$ volume-based hierarchical polynomials of Table III with three different zeroth-order curl-conforming functions. To guarantee basis function independence, the chosen zeroth-order basis factors cannot be associated with edges bounding the same face [2]. Similarly, the $p(p+1)$ elements of a p order hierarchical base associated with DoF internal to the triangular face $\mathcal{T}^2(\xi_a, \xi_b, \xi_c)$ (possibly, the $\xi_d = 0$ face bounding the tetrahedral element $\mathcal{T}^3$) are obtained by forming the product of the $p(p+1)/2$ face-based hierarchical polynomials of Table II with two zeroth-order curl-conforming functions associated

TABLE IV
CORRESPONDENCE BETWEEN DUMMY AND PARENT VARIABLES

Zeroth-order basis factor	$\{\xi_a, \xi_b, \xi_c, \xi_d\}$	Zeroth-order basis factor	$\{\xi_a, \xi_b, \xi_c, \xi_d\}$
$\mathbf{\Omega}_1$, $\mathbf{\Lambda}_1$	$\{\xi_2, \xi_3, \xi_1, 0\}$	$\mathbf{\Omega}_2$, $\mathbf{\Lambda}_2$	$\{\xi_3, \xi_1, \xi_2, 0\}$
$\mathbf{\Omega}_3$, $\mathbf{\Lambda}_3$	$\{\xi_1, \xi_2, \xi_3, 0\}$		
$\mathbf{\Omega}_{12}$	$\{\xi_3, \xi_4, \xi_1, \xi_2\}$	$\mathbf{\Omega}_{23}$	$\{\xi_1, \xi_4, \xi_2, \xi_3\}$
$\mathbf{\Omega}_{13}$	$\{\xi_4, \xi_2, \xi_1, \xi_3\}$	$\mathbf{\Omega}_{24}$	$\{\xi_3, \xi_1, \xi_2, \xi_4\}$
$\mathbf{\Omega}_{14}$	$\{\xi_2, \xi_3, \xi_1, \xi_4\}$	$\mathbf{\Omega}_{34}$	$\{\xi_1, \xi_2, \xi_3, \xi_4\}$

Hierarchical basis functions are the product of the polynomials of Tables II–III with the zeroth-order vector functions of [2] listed here in the left-hand columns. In forming the products, the dummy parent variables $\{\xi_a, \xi_b, \xi_c, \xi_d\}$ appearing in the polynomials reported in Tables II-III are replaced by the parent variables reported in the right-hand columns. The first two rows consider both the curl- ($\mathbf{\Omega}$) and the divergence-conforming ($\mathbf{\Lambda}$) triangular bases; in this case one has to set $\xi_d = 0$ in Table II. The last three rows hold for the curl-conforming bases of the tetrahedral element.

with two edges bounding $\mathcal{T}^2$. Finally, the $(p+1)$ elements of a p order hierarchical base associated with edge DoF relative to the edge $\mathcal{T}^1(\xi_a, \xi_b)$ (possibly, the $\xi_c = \xi_d = 0$ edge bounding the tetrahedral element $\mathcal{T}^3$, or the $\xi_c = 0$ edge bounding the triangular element $\mathcal{T}^2$) are obtained by forming the product of the $(p+1)$ edge-based hierarchical polynomials of Table II with the zeroth-order curl-conforming function along that edge. It is here understood that, in this construction process, the dummy parent variables $\{\xi_a, \xi_b, \xi_c, \xi_d\}$ appearing in the polynomial expressions reported in Tables II–III are replaced by the permutation of $\{\xi_1, \xi_2, \xi_3, \xi_4\}$ that corresponds to the appropriate zeroth-order basis factor shown in Table IV.

III. NUMERICAL RESULTS

A. Triangular Element

Consider the vector Helmholtz equation

$$\nabla \times \nabla \times \boldsymbol{H} = k^2 \boldsymbol{H} \tag{1}$$

representing a two-dimensional cavity bounded by perfectly conducting walls (a homogeneous Neumann boundary). For the magnetic field

$$\boldsymbol{H} = \sum_i \alpha_i \boldsymbol{B}_i \tag{2}$$

expressed in terms of vector basis functions $\boldsymbol{B}_i$, the element matrices $\mathbf{S}$ and $\mathbf{T}$ have entries of the form

$$\mathrm{S}_{mn} = \iint_S \nabla \times \boldsymbol{B}_m \cdot \nabla \times \boldsymbol{B}_n \, \mathrm{d}S \tag{3}$$

$$\mathrm{T}_{mn} = \iint_S \boldsymbol{B}_m \cdot \boldsymbol{B}_n \, \mathrm{d}S \tag{4}$$

with *vector-field solution* (2) linearly dependent on the expansion-coefficient array $\boldsymbol{\alpha} = [\alpha_i]$

$$\boldsymbol{h} = \mathbf{T}\,\boldsymbol{\alpha}; \quad \boldsymbol{\alpha} = \mathbf{T}^{-1}\,\boldsymbol{h} \tag{5}$$

and where $\mathbf{T}$ now refers to the global matrix; the entries of $\boldsymbol{h}$ are

$$h_i = \iint_S \boldsymbol{H} \cdot \boldsymbol{B}_i \, \mathrm{d}S. \tag{6}$$

TABLE V
CONDITION NUMBERS (CN) AND NUMBER OF ITERATIONS RELATIVE TO A DRIVEN 2D – CAVITY PROBLEM

Bases given in [ref.], year	CN of the global $\mathbf{T}$-matrix of order 468	CN of the complete system matrix $[\mathbf{S} - k^2\mathbf{T}]$ of order 465	Number of BCG iterations
[6], 1998 [7], 1999	37,168	558,044	2,181
[12], 2003	60,697	102,469	732
[13], 2004	59,655	102,469	803
[14], 2006	2,058	102,832	383
the present paper	459	33,254	262

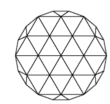

The problem is a circular TM cavity with PEC walls, modeled with 42 triangular cells (shown at left), using QT/CuN bases on triangles, which produced a system of order 465. Cell side lengths are a maximum of 0.15 wavelengths. One edge is driven with a constant tangential magnetic field. The number of iterations required by the biconjugate gradient algorithm (Jacobs' form) to reduce the residual error norm to 10^{-4} is reported in the right-hand column.

The linear independence of the basis set is an important attribute of a good basis. For example, the error $|\delta\boldsymbol{h}|$ of the vector-field solution depends on the error $\delta\alpha_i$ of each coefficient α_i appearing in (2) and, according to (5), the *confidence* in the numerical precision of the vector-field solution on equal residual error $|\delta\boldsymbol{\alpha}|$ clearly improves for decreasing condition number of the $\mathbf{T}$-matrix.

Because of the nullspace of the curl operator, the element matrix $\mathbf{S}$ is singular. However, $\mathbf{T}$ is nonsingular and its condition number (CN $= \|\mathbf{T}\|\,\|\mathbf{T}^{-1}\|$) provides a measure of the degree of linear independence of the basis functions, which in turn gives an indication of the performance of the basis functions in numerical applications. Similar comparisons of $\mathbf{T}$-matrix condition numbers were carried out in [21] for lower-order (linear tangential/ quadratic normal – LT/QN) basis functions; some higher-order comparisons are provided in [19].

Preliminary numerical results for triangular cells were previously published in [22], which compared the (element and global) $\mathbf{T}$-matrix condition numbers arising from several families of hierarchical vector basis functions to those of the new functions proposed here. That study, which treated the solution of (1) as an eigenvalue problem for the resonant frequencies of the cavity, concluded that the proposed basis functions of order 2.5 and 3.5 produce lower matrix condition numbers over a range of meshes than those of most other families. Those results were obtained after attempts were made to improve the condition numbers for the other families by an appropriate choice of scale factors.

Additional preliminary results for triangles are provided in Table V, which considers the matrix conditioning and iterative solution of the linear system associated with one example of a driven cavity described by (1). A constant magnetic field was imposed on one edge of the mesh, which contained reasonably well-controlled cell shapes, and quadratic tangential/cubic normal (QT/CuN) bases from several hierarchical families were employed. (These tests were carried out using the original scale factors provided by the authors of [6], [7], [12]–[14], and not

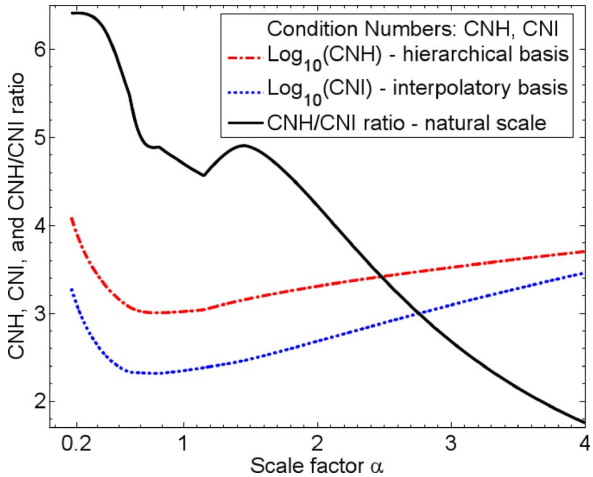

Fig. 2. Individual element $\mathbf{T}$-matrix condition numbers for the hierarchical (CNH) and the interpolatory (CNI) vector basis of order 2.5 obtained by considering tetrahedral cells of different height $\alpha\sqrt{6}\,\ell/3$, but with the same equilateral base of edge-length ℓ.

those introduced by the present authors in [22].) Table V shows that the conditioning of the overall system for the driven cavity is generally proportional to that of the global $\mathbf{T}$-matrix considered earlier. Table V also reports the number of iteration steps required to reduce the residual error norm to 10^{-4} using Jacobs' form of the biconjugate gradient algorithm [23], [24] without preconditioning. Diagonal matrix preconditioning was also considered and, for these test cases of relatively small matrix order, improved the performance of the solver for all of the basis function families (in fact, the preconditioned algorithm converged to the same residual with about the same amount of computation for each basis family except those of [6], [7], which required at least three times as many iterations). Similar results were observed as mesh quality degraded and other parameters were varied. While these results suggest that the new basis functions are at least as effective as existing bases when used with simple iterative solvers, we acknowledge that additional comparisons must be carried out before conclusions can be drawn about their performance in more realistic problems or with more sophisticated preconditioners.

B. Tetrahedral Element

As a preliminary evaluation of the tetrahedral bases, we compare the individual element $\mathbf{T}$-matrix condition number obtained using the 45 QT/CuN basis functions (of order 2.5) presented in this paper and the equivalent functions given in [2].

The best possible tetrahedral cell has equilateral shape, edge-length ℓ, and height $h = \sqrt{6}\,\ell/3$. Lower-quality cells may be obtained by scaling the height of this tetrahedron, thereby obtaining cells of different height $\alpha\, h$ and the same (equilateral) base. The element condition numbers CNH and CNI obtained with the hierarchical and the interpolatory family, respectively, depend on the value of α used to modify the cell shape; for these bases, however, the condition numbers CNH and CNI are not modified by changing the value of ℓ while keeping α fixed.

Fig. 2 shows the behavior of the condition numbers CNH and CNI for the two types of bases, and the ratio (CNH/CNI) of these two condition numbers, versus the scale factor α, for $0.15 \leq \alpha \leq 4$. These results show that, in case of rectilinear tetrahedral cells of good quality, and for element order 2.5, the individual element condition number CNH is expected to be four to five times larger than the individual element condition number CNI obtained with interpolatory polynomials. Conversely, for poor quality cells, the condition number obtained from the hierarchical vector bases could be much higher (say, by a factor of 7) than that obtained by using interpolatory polynomials; however, this result is still within an order of magnitude and cells of such poor quality are usually avoided whenever possible.

IV. CONCLUSION

A new family of hierarchical vector bases has been proposed for triangles and tetrahedra. The use of orthogonal scalar polynomials in their construction is believed to offer a simpler approach for enhancing their linear independence than the partial orthogonalization of the vector functions. Preliminary numerical results, presented here and in a companion paper [22], suggest that the new bases yield reasonably well-conditioned matrices.

APPENDIX
ORTHOGONAL POLYNOMIALS USED IN THE CONSTRUCTION OF HIERARCHICAL VECTOR BASES

In the first part of this Appendix (subsection A) we introduce and discuss auxiliary polynomials needed to construct hierarchical polynomial bases with terms subdivided into volume, face, and edge-based polynomials. The symbol used for these polynomials is related to their further use; that is, $\mathcal{V}$, $\mathcal{F}$, and $\mathcal{E}$ are the auxiliary polynomials used to construct the volume, the face, and the edge based polynomials, respectively. Then, the other three subsections of this Appendix (from B to D) show how to use the auxiliary polynomials to construct hierarchical volume, face, and edge-based polynomials called V, F, and E, respectively. In each group, the polynomials are mutually orthogonal independent of the definition domain of the inner product, i.e., either the volume, the face, or the edge of the element. This is a very important feature of our hierarchical bases because one can use the same polynomial bases either on tetrahedral, triangular or line elements, with no need to modify their expressions. The edge, face and volume-based polynomials are normalized as reported at the bottom of Table II–Table III; in numerical applications these polynomials can be normalized differently whenever convenient.

To compact the expressions of the polynomials of this Appendix it is convenient to introduce the following new variables

$$\begin{aligned} \xi_{ab} &= \xi_a - \xi_b \\ \xi_{cd} &= \xi_c - \xi_d \\ \chi_{ab} &= \xi_a + \xi_b \\ \chi_{cd} &= \xi_c + \xi_d \end{aligned} \tag{7}$$

with dependency relation

$$\chi_{ab} + \chi_{cd} = 1. \tag{8}$$

The expressions of the four parent variables $\{\xi_a, \xi_b, \xi_c, \xi_d\}$ in terms of the new dependent variables are straightforwardly obtained by inversion of (7).

A) Auxiliary Polynomials: Polynomials with particular symmetry properties in the dependent parent variables $\boldsymbol{\xi} = \{\xi_a, \xi_b, \xi_c, \xi_d\}$ used to describe the $T^1(\xi_a, \xi_b)$, the $T^2(\xi_a, \xi_b, \xi_c)$ and the $T^3(\xi_a, \xi_b, \xi_c, \xi_d)$ simplex are obtained by linear combinations of the Silvester (R_k) and the shifted Silvester ($\widehat{R}_k$) interpolatory polynomials given in [2]. For example, the pth order polynomials

$$\mathcal{E}_p(\xi_a, \xi_b) \underset{p\geq 0}{=} \sum_{i=1}^{i_{\max}} \beta_{p,i} \Big[\widehat{R}_{q-i}(q, \xi_a) \widehat{R}_i(q, \xi_b) + (-1)^p \widehat{R}_i(q, \xi_a) \widehat{R}_{q-i}(q, \xi_b) \Big] \quad (9)$$

with

$$q = p+2, \;\; i_{\max} = \begin{cases} \frac{q}{2}, & q \text{ even} \\ \frac{(q-1)}{2}, & q \text{ odd} \end{cases} \quad (10)$$

are either symmetric (for even or zero p values) or antisymmetric (for odd p values) in ξ_a and ξ_b, with $\mathcal{E}_p(\xi_b, \xi_a) = (-1)^p \; \mathcal{E}_p(\xi_a, \xi_b)$.

The coefficients $\beta_{p,i}$ in (9) are determined to define hierarchical polynomials associated with the edge $\xi_a + \xi_b = 1$. They are obtained by imposing, along the edge at issue (that is, the $T^1(\xi_a, \xi_b)$ simplex), the orthogonality of each $\mathcal{E}_p(\xi_a, \xi_b)$ with respect to all the polynomials $\mathcal{E}_m(\xi_a, \xi_b)$ of lower order m:

$$\int_0^1 \mathcal{E}_p(\xi_a, 1-\xi_a)\, \mathcal{E}_m(\xi_a, 1-\xi_a)\, \mathrm{d}\xi_a = \frac{\delta_{mp}}{2p+1} \quad (11)$$

where δ_{mp} is the Kronecker delta. The normalization (11) involves a unit constant weight function and makes $\mathcal{E}_p(\xi_a, 1-\xi_a)$ equal to the Shifted Legendre Polynomial $P_p^*(\xi_a)$. In principle, other normalizations with different weight functions are possible to make $\mathcal{E}_p$, for example, equal to Chebyshev or Jacobi polynomials. Convenient expressions for the $\mathcal{E}_p$ defined in (9) can be given in terms of the two new dependent variables ξ_{ab} and χ_{cd} given in (7). All the polynomials $\mathcal{E}_p$ are implicitly symmetric in the ξ_c and ξ_d variables since $\chi_{cd}(\xi_c, \xi_d) = \chi_{cd}(\xi_d, \xi_c) = \xi_c + \xi_d$.

In subsection C, to construct face-based polynomials, we also need the polynomials $\mathcal{F}_n(\xi_c)$ obtained by orthogonalizing the Silvester polynomials $R_n(p+2, \xi_c)$, for $n = 1, 2, \ldots, p$. All these polynomials contain a common factor ξ_c and do not have any symmetry or antisymmetry property in ξ_c, ξ_d because they are independent of ξ_d; they are normalized by setting

$$\iint_{T^2} \mathcal{F}_n(\xi_c)\, \mathcal{F}_m(\xi_c)\, \mathrm{d}T^2 = \frac{\delta_{mn}}{2n(n+1)(n+2)} \quad (12)$$

which yields $\mathcal{F}_n(1) = 1$ and $|\mathcal{F}_n(\xi_c)| \leq 1$ for $\{0 \leq \xi_c \leq 1\}$. These polynomials are obtained from the lowest order ones

$$\begin{cases} \mathcal{F}_1(\xi_c) &=& \xi_c \\ \mathcal{F}_2(\xi_c) &=& \xi_c \frac{(5\,\xi_c - 3)}{2} \end{cases} \quad (13)$$

by use of the following recurrence relations with respect to the degree n

$$a_{1n} \mathcal{F}_{n+1}(\xi_c) = (a_{2n}\xi_c - a_{3n}) \mathcal{F}_n(\xi_c) - a_{4n} \mathcal{F}_{n-1}(\xi_c) \quad (14)$$

with

$$\begin{cases} a_{1n} &=& (n+3)(2n+1) \\ a_{2n} &=& 2(2n+1)(2n+3) \\ a_{3n} &=& 2(2n^2+4n+3) \\ a_{4n} &=& (n-1)(2n+3) \end{cases} . \quad (15)$$

Orthogonal volume-based polynomials symmetric or antisymmetric in the (ξ_a, ξ_b) and the (ξ_c, ξ_d) variables can be obtained by linearly combining the Silvester and shifted Silvester interpolatory polynomials in a way similar to that used to get (9). To obtain these polynomials, however, it is much more convenient to start with expressions that involve the appropriate Legendre polynomials from the beginning. In fact, in subsection B of this Appendix, we use the following volume-based linearly independent polynomials of order $p = 2 + \ell + m + n$

$$\mathcal{V}_{\ell+2,m,n}(\xi_a, \xi_b, \xi_c, \xi_d) = \xi_c\, \xi_d\, \chi_{ab}^{\ell}\, P_m(\xi_{ab})\, P_n(\xi_{cd}) \quad (16)$$

which are symmetric in (ξ_a, ξ_b) and (ξ_c, ξ_d) for even values of m and n, respectively (antisymmetric otherwise), with

$$\begin{aligned} \mathcal{V}_{imn}(\xi_b, \xi_a, \xi_c, \xi_d) &= (-1)^m \; \mathcal{V}_{imn}(\xi_a, \xi_b, \xi_c, \xi_d) \\ \mathcal{V}_{imn}(\xi_a, \xi_b, \xi_d, \xi_c) &= (-1)^n \; \mathcal{V}_{imn}(\xi_a, \xi_b, \xi_c, \xi_d) \\ \mathcal{V}_{imn}(\xi_b, \xi_a, \xi_d, \xi_c) &= (-1)^{m+n} \; \mathcal{V}_{imn}(\xi_a, \xi_b, \xi_c, \xi_d). \end{aligned} \quad (17)$$

The integral of the product of a symmetric and an antisymmetric polynomial of the kind given in (9) automatically vanishes over the T^1, T^2, and T^3 simplex; similarly, the product of a symmetric and an antisymmetric polynomial of the kind given in (16) has a vanishing integral over T^3.

B) Volume-Based Hierarchical Polynomials Orthogonal Over T^3: In terms of the (dummy) parent variables used in the present paper, the $p(p^2-1)/6$ polynomials which in [2, Eq. (28)] interpolate internal points of the T^3 simplex read as follows:

$$\begin{aligned} I_{ijk\ell}(p, \xi_a, \xi_b, \xi_c, \xi_d) &= \widehat{R}_i(p+2, \xi_a) \widehat{R}_j(p+2, \xi_b) \\ &\quad \cdot R_k(p+2, \xi_c)\, R_\ell(p+2, \xi_d) \\ &\text{for } i,j = 1,2,\ldots,p+1\, ; \;\; k,\ell = 1,2,\ldots,p \\ &\quad i+j+k+\ell = p+2 \end{aligned} \quad (18)$$

and they vanish on the $\xi_c = 0$ and $\xi_d = 0$ faces because of the presence of a common $\xi_c\, \xi_d$ factor. According to our definition, the above polynomials are volume-based. An equivalent pth order hierarchical family consisting of $p(p^2-1)/6$ volume-based polynomials is obtained by applying the Gram-Schmidt orthogonalization process to the polynomial set (16), performed by using the Legendre inner product over the T^3 simplex. The hierarchical volume-based polynomials are thus obtained by orthogonalizing in order (from the first to the last polynomial) the list of the polynomials (16) provided by running a three nested loop: for $g = 2, 3, \ldots, p$ (outer loop on the *global* order $g = \ell + 2 + m + n$); $n = 0, 1, \ldots, g-2$, and order

$k=1 \quad \mathcal{E}_0(\xi_a,\xi_b)\,\mathcal{F}_1(\xi_c) = \mathcal{Q}_{01}(\xi_a,\xi_b,\xi_c)$

$k=2 \quad \mathcal{E}_0(\xi_a,\xi_b)\,\mathcal{F}_2(\xi_c) \rightarrow \mathcal{E}_1(\xi_a,\xi_b)\,\mathcal{F}_1(\xi_c)$

$k=3 \quad \mathcal{E}_0(\xi_a,\xi_b)\,\mathcal{F}_3(\xi_c) \rightarrow \mathcal{E}_1(\xi_a,\xi_b)\,\mathcal{F}_2(\xi_c) \rightarrow \mathcal{E}_2(\xi_a,\xi_b)\,\mathcal{F}_1(\xi_c)$

$k=4 \quad \mathcal{E}_0(\xi_a,\xi_b)\,\mathcal{F}_4(\xi_c) \rightarrow \mathcal{E}_1(\xi_a,\xi_b)\,\mathcal{F}_3(\xi_c) \rightarrow \mathcal{E}_2(\xi_a,\xi_b)\,\mathcal{F}_2(\xi_c) \rightarrow \mathcal{E}_3(\xi_a,\xi_b)\,\mathcal{F}_1(\xi_c)$

Fig. 3. Orthogonalization path followed by the two-nested loop used to build the face-based hierarchical polynomials $\mathcal{Q}_{mn}$. The outer loop is for $k=1,2,\ldots,p$; the inner loop is for $n=k,k-1,\ldots,1$. Thus, the kth order polynomial $\mathcal{Q}_{mn}$ (with $k=m+n$) is obtained by orthogonalizing $\mathcal{E}_m\,\mathcal{F}_n$ with respect to all the face-based orthogonal polynomials $\mathcal{Q}_{\jmath\ell}$ previously obtained up to the order $\jmath+\ell=k-1$ as well as, in the case of $m\geq 1$, by orthogonalizing $\mathcal{E}_m\,\mathcal{F}_n$ with respect to the polynomials $\mathcal{Q}_{\jmath\ell}$ previously obtained for $\jmath=0,1,\ldots,m-1$ with $\ell=k-\jmath$. The figure just shows the path from $k=1$ up to $k=4$. The procedure starts with $k=1$, where $\mathcal{Q}_{01}$ is known. For $k=2$ we first build $\mathcal{Q}_{02}$ by orthogonalizing $\mathcal{E}_0\,\mathcal{F}_2$ with respect to $\mathcal{Q}_{01}$, then we build $\mathcal{Q}_{11}$ by orthogonalizing $\mathcal{E}_1\,\mathcal{F}_1$ with respect to $\mathcal{Q}_{01}$ and $\mathcal{Q}_{02}$. For $k=3$ we first build $\mathcal{Q}_{03}$ by orthogonalizing $\mathcal{E}_0\,\mathcal{F}_3$ with respect to $\mathcal{Q}_{01}$, $\mathcal{Q}_{02}$, and $\mathcal{Q}_{11}$; then we build, in order, $\mathcal{Q}_{12}$ and $\mathcal{Q}_{21}$, etc.

$m=0,1,\ldots,g-2-n$ (inner loop), with $\ell=(g-2-m-n)$ (fixed in the inner loop).

The hierarchical polynomials $V_{ijk}(\boldsymbol{\xi})$ obtained in this manner are reported in Table III up to the sixth order. The global order of these polynomials is equal to $p=i+j+k$ and equivalently to the sum of the subscripts appearing in their expressions.

C) Face-Based Hierarchical Polynomials Orthogonal Over T^2 and T^3: In terms of the (dummy) parent variables used in the present paper, the $p(p+1)/2$ polynomials which in [2, Eqs. (10, 28)] interpolate the points located inside the triangular face described by the three parent variables ξ_a,ξ_b,ξ_c read as follows

$$\begin{aligned} I_{ijk}(p,\xi_a,\xi_b,\xi_c) &= \widehat{R}_i(p+2,\xi_a) \\ &\quad\cdot \widehat{R}_j(p+2,\xi_b)\,R_k(p+2,\xi_c) \\ &\quad \text{for } \; i,j=1,2,\ldots,p+1; \quad k=1,2,\ldots,p \\ &\quad \text{and } \; i+j+k=p+2. \end{aligned} \tag{19}$$

The $k=0$ case is here excluded since it yields edge-based functions that interpolate the $\xi_c=0$ edge of the triangle; those functions are considered in the following subsection D.

The face-based interpolatory polynomials (19) are replaced by hierarchical polynomials obtained by orthogonalizing in order over T^2, within a two-nested loop for $k=1,2,\ldots,p$ (outer loop) and $n=k,k-1,\ldots,1$ (inner loop; see Fig. 3), the kth order polynomials

$$\mathcal{P}_{mn}(\xi_a,\xi_b,\xi_c)=\mathcal{E}_m(\xi_a,\xi_b)\,\mathcal{F}_n(\xi_c) \tag{20}$$

where $k=m+n$ and with $\mathcal{E}_m$, $\mathcal{F}_n$ given in subsection A.

This orthogonalization process yields a polynomial set $\mathcal{Q}_{mn}(\xi_a,\xi_b,\xi_c)$ that contains all the *normalized* orthogonal polynomials $\mathcal{F}_n(\xi_c)$, with $\mathcal{Q}_{0n}(\xi_a,\xi_b,\xi_c)=\mathcal{F}_n(\xi_c)$, and $\mathcal{Q}_{0n}=1$ at $\xi_c=1$. The order of $\mathcal{Q}_{mn}$ is $(m+n)$ and coincides with the sum of the subscripts m and n of the $\mathcal{E}_m$ and $\mathcal{F}_n$ functions in (20). Furthermore, $\mathcal{Q}_{mn}$ is symmetric in ξ_a, ξ_b if m is even or equal to zero, whereas $\mathcal{Q}_{mn}$ is antisymmetric in ξ_a, ξ_b if m is odd.

The hierarchical polynomials $\mathcal{Q}_{mn}(\xi_a,\xi_b,\xi_c)$ and $\mathcal{Q}_{mn}(\xi_a,\xi_b,\xi_d)$ obtained by this procedure are mutually orthogonal *only* over the triangular simplex $T^2(\xi_a,\xi_b,\xi_c)$ and $T^2(\xi_a,\xi_b,\xi_d)$, respectively. The $\mathcal{Q}_{mn}(\xi_a,\xi_b,\xi_c)$ are face-based and nonzero on the triangular face $\xi_d=0$, and equal to zero at $\xi_c=0$ because of the presence of a common ξ_c factor. In order to obtain a hierarchical family of face-based polynomials $F_{mn}(\boldsymbol{\xi})$ mutually orthogonal on both the $T^2(\xi_a,\xi_b,\xi_c)$ and the T^3 simplex, it is sufficient to add to the polynomials $\mathcal{Q}_{mn}(\xi_a,\xi_b,\xi_c)$ an appropriate linear combination of the volume-based polynomials $V_p(\boldsymbol{\xi})$ (derived in subsection B) of global order p less than or equal to $(m+n)$, and which share the same symmetry properties of $\mathcal{Q}_{mn}$ with respect to the ξ_a and ξ_b variables. The $F_{mn}(\boldsymbol{\xi})$ polynomials define the following polynomials of global order $(m+n)$

$$\widetilde{\mathcal{E}}^{s|a,s}_{m+n}(\boldsymbol{\xi})=F^{s|a}_{mn}(\xi_a,\xi_b,\xi_c,\xi_d)+F^{s|a}_{mn}(\xi_a,\xi_b,\xi_d,\xi_c) \tag{21}$$

used in subsection D to construct edge-based polynomials symmetric in the ξ_c and ξ_d variables, and orthogonal on the $T^2(\xi_a,\xi_b,\xi_c)$, the $T^2(\xi_a,\xi_b,\xi_d)$, and the T^3 simplices.

Table II reports, up to the sixth order, the normalized face-based hierarchical polynomials $F_{mn}(\boldsymbol{\xi})$ for the T^2 and T^3 simplices.

D) Edge-Based Hierarchical Polynomials Orthogonal Over T^1, T^2 and T^3: In terms of the (dummy) parent variables used in the present paper, the $(p+1)$ polynomials which in [2, Eqs. (10), (28)] interpolate the edge described by the two parent variables ξ_a, ξ_b read as follows

$$\begin{aligned} I_{ij}(p,\xi_a,\xi_b) &= \widehat{R}_i(p+2,\xi_a)\,\widehat{R}_j(p+2,\xi_b) \\ &\quad \text{for } \; i,j=1,2,\ldots,p+1 \\ &\quad \text{and } \; i+j=p+2 \end{aligned} \tag{22}$$

and could be substituted with the hierarchical polynomials $\mathcal{E}_p(\xi_a,\xi_b)=\mathcal{E}_p(\xi_{ab},\chi_{cd})$ of subsection A.

The hierarchical polynomials for the line element (that is, the T^1 simplex) are simply obtained from $\mathcal{E}_p(\xi_{ab},\chi_{cd})$ by setting $\chi_{cd}=0$, which is equivalent to set $\xi_a+\xi_b=1$. In the line-element case the functions $\mathcal{E}_p$ are easily obtained by the recurrence relation available in [25], since $\mathcal{E}_p(\chi_{cd}=0)$ coincides by construction with the Legendre polynomial $P_p(\xi_{ab})$ or, equivalently, with the Shifted Legendre polynomial $P^*_p(\xi_a)$.

However, unfortunately, the edge-based hierarchical polynomials $\mathcal{E}_p$ are mutually orthogonal *only* over the simplex T^1. In order to obtain a hierarchical family of edge-based polynomials symmetric in the ξ_c and ξ_d variables, and mutually orthogonal also on the $T^3(\xi_a,\xi_b,\xi_c,\xi_d)$ simplex, the $T^2(\xi_a,\xi_b,\xi_c)$ simplex (where $\xi_d = 0$), and the $T^2(\xi_a, \xi_b, \xi_d)$ simplex (where $\xi_c = 0$), it is sufficient to add to the pth order polynomial $\mathcal{E}_p$ an appropriate linear combination of the polynomials $\widetilde{\mathcal{E}}_m$ of subsection C (given in (21)), and of the volume-based polynomials $V_m(\boldsymbol{\xi})$ of subsection B, which share the same symmetry properties of $\mathcal{E}_p$ with respect to the four parent variables. All the polynomials involved in this combination are of order $m \leq p$. Notice also that the linear combination at issue here involves only those volume-based polynomials that are symmetric with respect to the ξ_c and ξ_d variables.

The hierarchical polynomials E_p obtained in this manner are reported in Table II, up to the sixth order.

E) Distinguishing Features of the New Polynomial Bases: As previously discussed in this Appendix, in general, a polynomial of one group (either the volume, the face, or the edge-based group) is not orthogonal to a polynomial of a different group, but all the polynomials within each group are mutually orthogonal independent of the definition domain of the Legendre inner product (i.e., either the volume, the face, or the edge of the element). This feature is readily appreciated if one considers the Gram matrix M_p having coefficient M_{ij} equal to the Legendre inner product (on the T^1, T^2, or T^3 simplex) of the ith and jth polynomials of the pth–order-complete family, see [18, Fig. 3]. As shown in [18], for $p \geq 3$, the condition numbers of the M_p matrices obtained by using our hierarchical polynomial bases are lower than those obtained by using the Silvester-Legendre interpolatory polynomials.

REFERENCES

[1] J. C. Nédélec, “Mixed finite elements in R3,” *Num. Math.*, vol. 35, pp. 315–341, 1980.

[2] R. D. Graglia, D. R. Wilton, and A. F. Peterson, “Higher order interpolatory vector bases for computational electromagnetics, special issue on “Advanced numerical techniques in electromagnetics”,” *IEEE Trans. Antennas Propag.*, vol. 45, pp. 329–342, Mar. 1997.

[3] J. P. Webb and B. Forghani, “Hierarchal scalar and vector tetrahedra,” *IEEE Trans. Magn.*, vol. 29, pp. 1495–1498, Mar. 1993.

[4] C. Carrié and J. P. Webb, “Hierarchal triangular edge elements using orthogonal polynomials,” in *Proc. IEEE Int. Antennas Propagation Symp.*, Montreal, Jul. 1997, vol. 2, pp. 1301–1313.

[5] J. Wang and J. P. Webb, “Hierarchal vector boundary elements and p-adaption for 3D electromagnetic scattering,” *IEEE Trans. Antennas Propag.*, vol. 45, no. 12, pp. 1869–1879, Dec. 1997.

[6] L. S. Andersen and J. L. Volakis, “Hierarchical tangential vector finite elements for tetrahedra,” *IEEE Microw. Guided Wave Lett.*, vol. 8, no. 3, pp. 127–129, Mar. 1998.

[7] L. S. Andersen and J. L. Volakis, “Development and application of a novel class of hierarchical tangential vector finite elements for electromagnetics,” *IEEE Trans. Antennas Propag.*, vol. 47, no. 1, pp. 112–120, Jan. 1999.

[8] J. P. Webb, “Hierarchal vector basis functions of arbitrary order for triangular and tetrahedral finite elements,” *IEEE Trans. Antennas Propag.*, vol. 47, no. 8, pp. 1244–1253, Aug. 1999.

[9] D. K. Sun, J. F. Lee, and Z. Cendes, “Construction of nearly orthogonal Nedelec bases for rapid convergence with multilevel preconditioned solvers,” *SIAM J. Sci. Comput.*, vol. 23, no. 4, pp. 1053–1076, 2001.

[10] M. Ainsworth and J. Coyle, “Hierarchic hp-edge element families for Maxwell’s equations on hybrid quadrilateral/triangular meshes,” *Comput. Methods Appl. Mech. Engng.*, vol. 190, pp. 6709–6733, 2001.

[11] M. Ainsworth and J. Coyle, “Hierarchic finite element bases on unstructured tetrahedral meshes,” *Int. J. Numer. Meth. Engng.*, vol. 58, no. 14, pp. 2103–2130, Dec. 14, 2003.

[12] S. C. Lee, J. F. Lee, and R. Lee, “Hierarchical vector finite elements for analyzing waveguiding structures,” *IEEE Trans. Antennas Propag.*, vol. 51, pp. 1897–1905, Aug. 2003.

[13] R. S. Preissig and A. F. Peterson, “A rationale for p-refinement with vector finite elements,” *Appl. Computat. Electromagn. Soc. (ACES) J.*, vol. 19, pp. 65–75, Jul. 2004.

[14] P. Ingelström, “A new set of h(curl)-conforming hierarchical basis functions for tetrahedral meshes,” *IEEE Trans. Microw. Theory Tech.*, vol. 54, no. 1, pp. 106–114, Jan. 2006.

[15] J. Schöberl and S. Zaglmayr, “High order Nédélec elements with local complete sequence properties,” *Int. J. Comput. Math. Electr. Electron. Eng. (COMPEL)*, vol. 24, no. 2, pp. 374–384, 2005.

[16] S. Zaglmayr, “High order finite element methods for electromagnetic field computation,” Ph.D. dissertation, Johannes Kepler Universität, Linz, Austria, 2006.

[17] R. D. Graglia and A. F. Peterson, “Fully conforming hierarchical vector bases for finite methods,” presented at the URSI Nat. Radio Sci. Meeting, Charleston, SC, Jun. 1–5, 2009.

[18] R. D. Graglia, A. F. Peterson, and F. P. Andriulli, “Hierarchical polynomials and vector elements for finite methods,” in *Proc. Int. Conf. Electromagn. Adv. Applicat. (ICEAA 2009)*, Torino, Italy, Sep. 2009, vol. 1, pp. 1086–1089, doi: 10.1109/ICEAA.2009.5297791.

[19] R. Abdul-Rahman and M. Kasper, “Orthogonal hierarchical Nédélec elements,” *IEEE Trans. Magn.*, vol. 44, pp. 1210–1213, Jun. 2008.

[20] J. P. Webb, “Matching a given field using hierarchal vector basis functions,” *Electromagnetics*, vol. 24, no. 1-2, pp. 113–122, Jan. 1, 2004.

[21] L. S. Andersen and J. L. Volakis, “Condition numbers for various FEM matrices,” *J. Electromagn. Waves Appl.*, vol. 13, no. 12, pp. 1663–1679, Jan. 1, 1999.

[22] A. F. Peterson and R. D. Graglia, “Scale factors and matrix conditioning associated with triangular-cell hierarchical vector basis functions,” *IEEE Antennas Wireless Propag. Lett.*, vol. 9, pp. 40–43, 2010.

[23] D. A. H. Jacobs, , I. S. Duff, Ed., “The exploitation of sparsity by iterative methods,” in *Sparse Matrices and Their Uses*. Berlin: Springer-Verlag, 1981, pp. 191–222.

[24] C. F. Smith, A. F. Peterson, and R. Mittra, “The biconjugate gradient method for electromagnetic scattering,” *IEEE Trans. Antennas Propag.*, vol. 38, no. 6, pp. 938–940, Jun 1990.

[25] M. Abramowitz and I. A. Stegun, *Handbook of Mathematical Functions*. New York: Dover, 1968.

Roberto D. Graglia (S’83–M’83–SM’90–F’98) was born in Turin, Italy, on July 6, 1955. He received the Laurea degree (*summa cum laude*) in electronic engineering from the Polytechnic of Turin, in 1979 and the Ph.D. degree in electrical engineering and computer science from the University of Illinois at Chicago, in 1983.

From 1980 to 1981, he was a Research Engineer at CSELT, Italy, where he conducted research on microstrip circuits. From 1981 to 1983, he was a Teaching and Research Assistant at the University of Illinois at Chicago. From 1985 to 1992, he was a Researcher with the Italian National Research Council (CNR), where he supervised international research projects. In 1991 and 1993, he was Associate Visiting Professor at the University of Illinois at Chicago. In 1992, he joined the Department of Electronics, Polytechnic of Turin, as an Associate Professor and has been a Professor in the Electrical Engineering Department since 1999. He has authored over 150 publications in international scientific journals and symposia proceedings. His areas of interest comprise numerical methods for high- and low-frequency electromagnetics, theoretical and computational aspects of scattering and interactions with complex media, waveguides, antennas, electromagnetic compatibility, and low-frequency phenomena. He has organized and offered several short courses in these areas.

Dr. Graglia has been a Member of the editorial board of ELECTROMAGNETICS since 1997. He is a past Associate Editor of the IEEE TRANSACTIONS ON ANTENNAS AND PROPAGATION and the IEEE TRANSACTIONS ON ELECTROMAGNETIC COMPATIBILITY. He is currently an Associate Editor of the IEEE ANTENNAS AND WIRELESS PROPAGATION LETTERS and a Reviewer for several international journals. He was the Guest Editor of a special issue on Advanced Numerical Techniques in Electromagnetics for the IEEE TRANSACTIONS ON ANTENNAS AND PROPAGATION in March 1997. He has been Invited Convener at URSI General Assemblies for special sessions on Field and Waves in 1996, Electromagnetic Metrology in 1999, and Computational Electromagnetics in 1999. He served the International Union of Radio Science (URSI) for the triennial International Symposia on Electromagnetic Theory as Organizer of the Special Session on Electromagnetic Compatibility in 1998 and was the co-organizer of the special session on Numerical Methods in 2004. Since 1999, he has been the General Chairperson of the International Conference on Electromagnetics in Advanced Applications (ICEAA). He has been a member of the AP-S Administrative Committee for the triennium 2006–2008 and is presently an AP-S Distinguished Lecturer (2009–2012).

Andrew F. Peterson (S'82–M'83–SM'92–F'00) received the B.S., M.S., and Ph.D. degrees in electrical engineering from the University of Illinois at Urbana-Champaign, in 1982, 1983, and 1986, respectively.

Since 1989, he has been a member of the faculty of the School of Electrical and Computer Engineering, Georgia Institute of Technology, Atlanta, where he is now Professor and Associate Chair for Faculty Development. He teaches electromagnetic field theory and computational electromagnetics, and conducts research in the development of computational techniques for electromagnetic scattering, microwave devices, and electronic packaging applications. He is the principal author of *Computational Methods for Electromagnetics* (IEEE Press, 1998).

Dr. Peterson is a past recipient of the ONR Graduate Fellowship and the NSF Young Investigator Award. He has served as an Associate Editor of the IEEE TRANSACTIONS ON ANTENNAS AND PROPAGATION, the *IEEE Antennas and Wireless Propagation Letters*, as the General Chair of the 1998 IEEE AP-S International Symposium and URSI/USNC Radio Science Meeting, and as a member of IEEE AP-S AdCom. He also served for six years as a Director of ACES, and two years as Chair of the IEEE Atlanta Section. He was the President of the IEEE AP-S during 2006. He is a recipient of the IEEE Third Millennium Medal. He is also a Fellow of the Applied Computational Electromagnetics Society (ACES), and a member of the International Union of Radio Scientists (URSI) Commission B, the American Society for Engineering Education, and the American Association of University Professors.

Francesco P. Andriulli (S'05–M'09) received the Laurea degree in electrical engineering from the Politecnico di Torino, Italy, in 2004, the M.S. degree in electrical engineering and computer science from the University of Illinois at Chicago in 2004, and the Ph.D. degree in electrical engineering from the University of Michigan at Ann Arbor in 2008.

From 2008 to 2010, he was a Research Associate with the Politecnico di Torino. Since 2010 he has been with the Microwave Department, École nationale supérieure des télécommunications de Bretagne (TELECOM Bretagne), Brest, France, where he is currently a Maître de conférences. His research interests are in computational electromagnetics with focus on preconditioning and fast solution of frequency and time domain integral equations, integral equation theory, hierarchical techniques, and single source integral equations.

Dr. Andriulli was awarded the University of Michigan International Student Fellowship and the University of Michigan Horace H. Rackham Predoctoral Fellowship. He was the recipient of the best student paper award at the 2007 URSI North American Radio Science Meeting. He received the first place prize of the student paper context of the 2008 IEEE Antennas and Propagation Society International Symposium, where he authored and coauthored other two finalist papers. He was the recipient of the 2009 RMTG Award for junior researchers and was awarded a URSI Young Scientist Award at the 2010 International Symposium on Electromagnetic Theory.